Investigating unsteady secondary flows in a linear low pressure turbine cascade: A combined experimental and numerical study

R. Ciorciari - I. Kirik - R. Niehuis

Institute of Jet Propulsion
Universitaet der Bundeswehr Muenchen
Werner-Heiseberg-Weg 39
85577 Neubiberg, Germany
Email: roberto.ciorciari@unibw.de

ABSTRACT

The effects of unsteady incoming wakes on the secondary flow in a linear low pressure turbine cascade, named T106, were investigated by experiments in a high speed cascade wind tunnel and by U-RANS simulations. In this paper, results of a variety of cases with different Strouhal numbers and flow coefficients were compared and the differences analysed.

The upstream incoming wakes in the experiment were generated by a wake generator and were considered in the CFD simulations likewise. The computations have been conducted using the flow solver TRACE. Time-averaged and time-accurate ensemble averaged experimental data permit the evaluation of the numerical U-RANS predictions for some of the investigated configurations. 3D CTA hot-wire traverses downstream the cascade permit to analyse the velocity and the turbulent flow field for the investigated configurations. Results of a newly implemented fast response total pressure probe allow to compare the relative unsteady ensemble averaged fluctuations to the CFD results downstream of the cascade.

NOMENCLATURE

Latin Symbols

c	chord
C_s	first Sutherland constant
C_{st}	second Sutherland constant
H	blade span
h	half blade span , $H/2$
Ma	Mach number
p	pressure
q	dynamic pressure
R	universal gas constant
Re	Reynolds number
Sr	Strouhal number, $(v_b/t_b) \cdot (c/v_{ax0})$
T	temperature, bar passing period, t_b/v_b
t	pitch, time
Tu	turbulence intensity
v	velocity
x	axial coordinate
$y, u/t$	pitch-wise coordinate
$z, z/h$	span-wise coordinate

Greek Symbols

α	span-wise angle
β	yaw (pitch-wise) angle
$\Delta p_t/q_{2th}$	total pressure losses, $(p_{t0} - p_{t2})/q_{2th}$
κ	specific heat capacity ratio
λ	thermal conductivity
ϕ	flow coefficient,v_{ax}/v_b
ω	vorticity

Abbreviations

CFD	Computational Fluid Dynamics
CV	Corner Vortex
EXP	Experimental
LPT	Low Pressure Turbine
MDPP	Moving Domain Passing Period
PV	Passage Vortex
SVO	Streamwise Vorticity
TEWV	Trailing Edge Wake Vortex

subscripts

0,1,2	measurement planes
ax	axial
abs	absolute
b	bar
k	relative to the pressure chamber
rel	relative
t	total
th	theoretical
sec	secondary

INTRODUCTION

The effects of unsteady incoming wakes on downstream profile losses (at midspan) were investigated at typical passing frequencies and wake strength in numerous studies (Acton, 1998; Stadtmueller, 2002; Schobeiri et al., 2003; Coton, 2004; Hodson and Howell, 2005; Schwarze and Niehuis, 2010; Pacciani et al., 2012). The wake-induced boundary layer transition shows the possibility to prevent large aerodynamic losses at low Reynolds numbers, to control the flow separation behaviour and consequently the profile losses. Recent thermodynamic investigations of wake blade interaction in an axial flow turbine were performed by Rose et al.(2013), through experiments and a 2D U-RANS simulations.

Further looking at the entire span-height and at the endwalls, the passing wakes generate an unsteady flow field and influence the inlet boundary layer which could affect the generation and development of the secondary flows and the relative losses. Renaud in his doctoral thesis (Renaud, 1991) presents an investigation about the effects of circumferential distortion of the inflow on the secondary flows downstream of a turbine rotor. He observed in his experiments that the rotor exit flow shows a periodical variation related to the relative vane passing frequency which influences the secondary flows. Interaction effects of stator and rotor aerofoils in a 1.5 stage axial turbine were investigated by Reinmoeller et al.(2002) and Reinmoeller (2007) through experiments and with the support of CFD. The influence of the first stator wake is detected downstream the rotor by time-averaged and time-accurate flow parameters taking into account relative clocking effects of the downstream stator.

An overview of endwall flow losses in axial turbine was published by Lampart (2009 a). First he summarises the formation process of endwall flows and then he proceeds with a description of the endwall loss analysis by an entropy generation function. In the second part (Lampart, 2009 b), he presents the effects of geometrical and flow parameters by CFD results. He makes a clear distinction between secondary flow development in cascade with and without tip clearance. Finally, he also indicates that the transport of upstream two dimensional wakes leads to oscillations of the secondary flows in the downstream passage. He explains these periodical variations by local changes of the inflow angle during the time of interaction with the passing wakes.

Casciaro et al. (2000) investigated the effects of incoming wakes on the secondary flow in axial turbines by two bar-blade configurations. The first was characterised by a distance of the bar from the leading edge of 50% of the true chord and the second by a distance of 25%. Both were computed with a U-RANS solver in 2D and 3D, using a $k-\epsilon$ two equation turbulence model. Stronger wake decay was observed in the calculation with respect to theoretical values. For both bar-blade configurations the physics observed in the research was the same, so it was believed to be independent of the wake decay. The secondary flow structures were stable in time, only small fluctuations were produced by the periodical incoming wakes. Unsteady secondary flows measurements in a high pressure turbine cascade, induced by upstream moving bars, were presented by Volino et al. (2013). The velocities, the turbulence levels, and turbulence spectra downstream of the bars and the cascade aerofoils are shown. Reynolds numbers of 30k and 60k, based on the inlet velocity, with and without incoming wakes were investigated in a low speed wind tunnel. The measured total pressure losses show very small differences between the two different Reynolds numbers and between the 30k case with and without incoming wakes, concerning the time-averaged results.

In the last decades, the results obtained by measurements and simulations in linear turbine cascades have given a fundamental contribution to better understand the complex flows in turbomachinery. Detailed experimental investigations of specific aerodynamic phenomena in cascades are also very useful to validate results obtained by advanced CFD codes. In the present paper the unsteady secondary flows produced by periodic incoming wakes in a low pressure turbine cascade are analysed by results obtained by CFD predictions. The aim is to give a contribution to better understanding the complex 3D unsteady flow mechanisms inside and downstream the cascade. A good prediction capability of the basic time-averaged and time-accurate ensemble averaged flow parameters through the used numerical model was observed in a previous investigation (Ciorciari et al., 2014). In this paper additional comparisons between experiments and CFD are presented. Different configurations, characterised by incoming wakes with different Strouhal numbers and flow coefficients, are also investigated with U-RANS to describe the time-averaged secondary flow features and the unsteady flow properties downstream the cascade.

EXPERIMENTAL TEST FACILITY AND TECHNIQUES

The High Speed Cascade Wind Tunnel of the Institute of Jet Propulsion of the University of the German Federal Armed Forces Munich (Universitaet der Bundeswehr Muenchen) is a continuously operating open-loop test facility located inside a cylindrical pressure chamber, allowing to set up independently Mach and Reynolds numbers. It is described in detail by Sturm and Fottner (1985). All measurements presented in this paper were taken in this test facility.

The flow parameters for all the configurations presented in this paper are a theoretical exit Mach number $Ma_{2th} = 0.59$ and Reynolds number $Re_{2th} = 2 \cdot 10^5$, calculated with the following relations:

$$Ma_{2th} = \sqrt{\frac{2}{\kappa - 1}\left(\left(\frac{p_{t1}}{p_k}\right)^{\frac{\kappa-1}{\kappa}} - 1\right)} \tag{1}$$

$$Re_{2th} = \sqrt{\frac{\kappa}{R}} \cdot \frac{c}{C_{st}} \cdot \frac{Ma_{2th} \cdot p_k \cdot \left(\frac{T_{t0}}{1+\left(\frac{\kappa-1}{2}\right)\cdot Ma_{2th}^2} + C_s\right)}{\left(\frac{T_{t0}}{1+\left(\frac{\kappa-1}{2}\right)\cdot Ma_{2th}^2}\right)^2} \tag{2}$$

The total inlet temperature T_{t0} and pressure P_{t0}, the static chamber pressure p_k and the aerofoil chord c are measured. The kinematic viscosity is calculated by the Sutherland‘s law with the constants $C_{st} = 1.458 \cdot 10^{-6} kg/(ms\sqrt{K})$ and $C_s = 110.4K$ (Ladwig, 1991). The specific air constant R and the ratio of specific heat $\kappa = c_p/c_v$ are assumed constant, respectively 287 J/(kg K) and 1.4. In order to set the operation point, the exit (or chamber) pressure p_k was measured in a calmed region inside the pressure chamber.

Three relevant axial measurements planes were defined, Fig. 1. Measurement plane 0, in front of the moving bars, where the stagnation pressure p_{t0} of the inflow is measured by a pitot probe at about 50 mm from the nozzle side wall. The inlet stagnation temperature T_{t0} was measured in the settling chamber using four PT100 class A platinum resistance temperature detectors. Heat transfer between the settling chamber and test section is neglected consequently T_{t0} is the assumed total temperature at this plane. Measurement plane 1 is located downstream the moving bars, approximately 77% chord length upstream the cascade leading edge and the moving bars approximately 83%. A triple hot-wire and a pitot probe were used there to measure the cascade inflow conditions. Finally, measurement plane 2 located 40% chord length downstream the aerofoil trailing edges. In this plane a five-hole probe, a triple hot-wire probe, and a fast response total pressure probe were used to obtain time-averaged and time-accurate (ensemble averaged) validation data. A proper reference for all the new

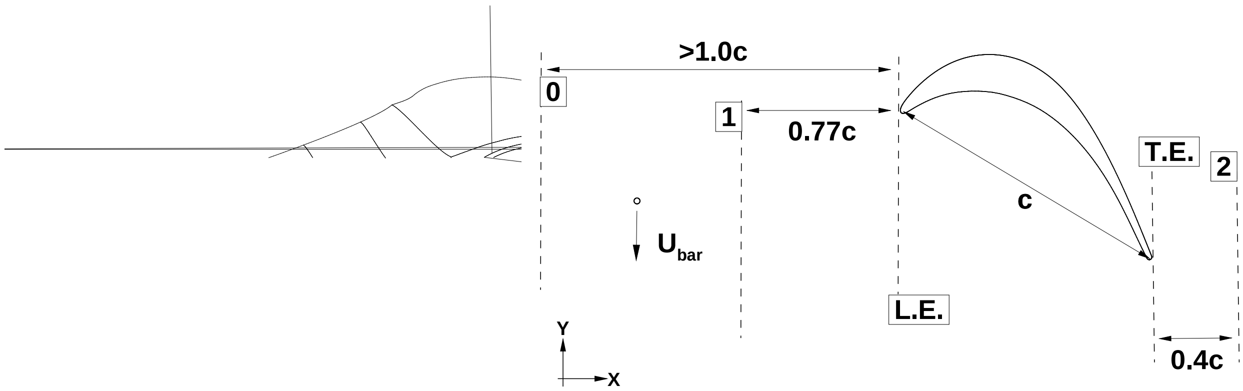

>1.0c
0
1
0.77c
c
T.E.
2
U bar
L.E.
Y
X
0.4c

Conf.	$t_b[mm]$	$v_b[m/s]$	$\phi[-]$	$Sr[-]$	EXP	CFD
T40 10	40	10	7.6	0.33	x	x
T40 20	40	20	3.8	0.66	x	x
T80 20	80	20	3.8	0.33	x	x
T80 40	80	40	1.9	0.66	-	x
T80 80	80	80	0.9	1.32	-	x

Table 1: **Configurations under consideration here**

NUMERICAL METHODOLOGY

Flow solver and domain discretisation

The flow solver TRACE has been used for all the simulations presented here. It is developed by DLR Cologne, Institute of Propulsion Technology in collaboration with MTU Aero-Engines. The code solves the unsteady Reynolds Averaged Navier-Stokes equations using a finite volume approach. More information and details on the flow solver TRACE can be found in open literature (Engel, 1997; Eulitz, 2000; Yang et al., 2002; Yang et al., 2006).
In the present work the RANS turbulent closure is modelled using the Wilcox $k-\omega$ two equations turbulence model, including the additional Kato and Launder pressure stagnation anomally fix (Kato and Launder, 1993; Kozulovic et al., 2004). The transition model used in this work is the $\gamma - Re_{\theta t}$ transport equation model (Marciniak et al., 2010; Menter and Langtry, 2004; Langtry and Menter, 2004). A Low-Reynolds approach is used and the non-dimensional wall distances are smaller than 1 at all viscous solid walls. More details about the numerical set-up and the domain discretisation are available in Ciorciari et al.(2014).

Boundary conditions

A midspan symmetrical 3D numerical model domain was used in the calculations. In pitch-wise direction, translational periodic boundary conditions were applied. Adiabatic no-slip conditions were used on solid walls and an inviscid wall was used only for the lower boundary on the moving bar domain, Fig. 1. The transition model was activated at all viscous boundaries. In all cases under consideration here, total pressure, total temperature, and turbulence intensity at the inlet have been set to the measured values obtained for the configuration without moving bars upstream of the cascade. The turbulent length scale at the inlet is of the order of 1% of the chord length.
In the steady cascade calculations, the inlet flow angle $\beta_{1steady}$ has been iteratively adjusted starting from the design angle ($\beta_{1design} = 127.7°$). A pressure sided incidence angle of $2°$ is needed to match the steady profile and the endwall static pressure distribution measured with installed wake generator without bars best. The same inlet angle was then used for all unsteady calculations in the plane upstream the wake generator ($\beta_0 = \beta_{1steady} = 129.7°$). This approach was preferred for the calculations for a better comparison between steady and unsteady cases and considering possible uncertainties of the hot-wire measurements at the inlet with the mounted wake generator. The measured static chamber pressure p_k and radial equilibrium conditions were imposed at the outlet plane. Furthermore non-reflecting boundary conditions were applied at the inlet and outlet planes.

Convergence criterion and time resolution

The convergence stopping criterion for the iterative steady calculations was established when the relative mass flow errors were less or equal to 10^{-6} and the average density residual reaches values smaller than 10^{-7}. For the unsteady sliding mesh calculations the time averaged mass flow differences for the unsteady computations are less than 10^{-4} and the average density residual reaches values less than 10^{-8}. A minimum time resolution of 800 time steps per moving domain passing period (MDPP), the inverse of the domain passing frequency, was used. The high time resolution was selected to resolve the high vortex shedding frequencies of the bars, which is of the order of 10kHz.

Secondary flow definition and evaluation parameters

In order to analyse the secondary flows in the cascade for the different CFD configurations, a 3D primary reference flow was defined by a steady computation with an inviscid endwall and an uniform inlet flow without boundary layer vorticity. Through the subtraction of this primary flow from the time-averaged predictions in each element of the numerical domain, the so-called secondary flow (sec) was obtained. The resulting secondary flows with the relative secondary velocity components were used to quantify the secondary flow features for the different configurations.
The following definition for the non-dimensionalised secondary streamwise vorticity (SVO_n) is used for all the numerical results presented here:

$$SVO_n = ((\omega_{xsec} \cdot v_{xsec}) + (\omega_{ysec} \cdot v_{ysec}) + (\omega_{zsec} \cdot v_{zsec})) \cdot c/v_{2mean} \tag{3}$$

The non-dimensionalised values are obtained through the multiplication of the ratio of the aerofoil chord c and the mean velocity v_{2mean} in the measurement plane 2 of the CFD steady configuration.

Results

Comparison with measured data (validation)

Time-averaged and time-accurate ensemble averaged experimental data, obtained with extensive measurement campaigns, have been used to evaluate the reliability of the numerical results. First the modelled 3D steady cascade flow without incoming wakes was compared to experimental results. The comparison of the profile and endwall pressure distributions between CFD and experiment shows a satisfying agreement. Small differences were observed in the diffusion region on the suction side, where a larger separation bubble was predicted with respect to the experiment (Ciorciari et al., 2014). For the periodic unsteady inflow, the velocity deficit, the turbulence level, and the inflow angle variations were used as validation parameters at the inlet to verify the numerically modelled incoming wakes. Downstream of the cascade, time-averaged and time-accurate secondary flow parameters were used to assess the CFD model. The numerical model reproduces reliably the main secondary flow features for the different investigated unsteady configurations. Details on these first validation steps were published by Ciorciari et al. (2014).

Comparison with unsteady triple hot-wire data in measurement plane 2

Velocity and turbulence intensity information were obtained with a triple hot wire probe. In the above mentioned work (Ciorciari et al., 2014), the velocity data permitted a comparison between the experimental and the CFD results of the span-wise distribution of the pitch-wise averaged $\Delta\beta_{2sec}$ over time downstream the cascade. Moderate periodical fluctuations of underturning and overturning, caused by the incoming wakes, were observed.
In Fig. 2 on the left, the distribution of the experimental ensemble averaged turbulence intensity values (a), in the measurement plane 2, for the T80 20 configuration is compared to the CFD predictions (b). Respective time-averaged velocity fields are plotted on the right of the same figure, in (c) and (d). The velocity values are non-dimensionalised by the mean velocity values in the respective measurement plane. The highest turbulence intensity values are visible in secondary flow and in the blade wake region. As can be seen, the CFD are able to reproduce the position and the extension of the secondary flow region like observed in the experiments. Differences were observed in the free-stream region where the predicted turbulence intensity values are smaller and in the wake turbulent diffusion region.

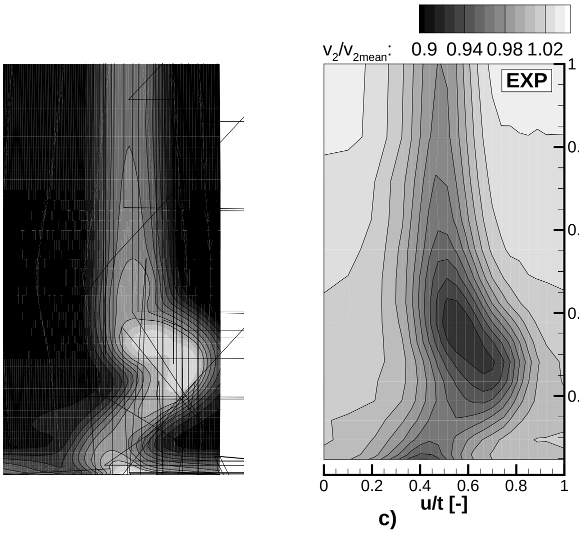

c)

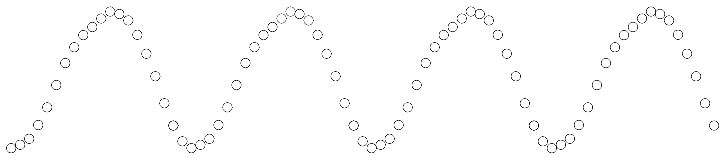

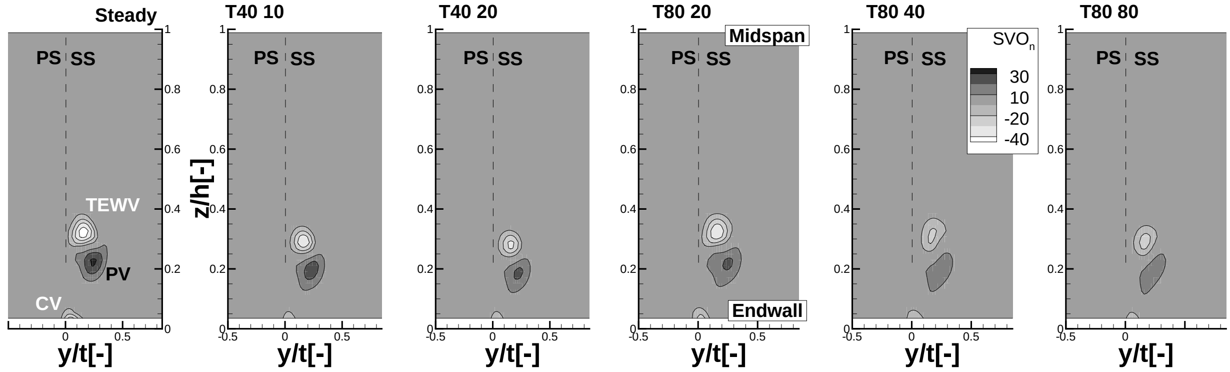

Figure 7: **Time-averaged SVO_n distributions downstream the cascade for the investigated configurations in measurement plane 2. (The dashed line shows the blade wake location)**

the steady one and a reduction of the standard deviation (St.dev.) are observed. The smaller standard deviation values indicate a more uniform distribution around the mean SVO_n values, which is around zero for all the configurations. The variations of the time-averaged inflow angles predicted in measurement plane 1 (Tab. 2) show the reduction of the incidence for the unsteady configurations respect to the steady one. For the configurations investigated here, this cause small effects on the cascade blade-to-blade inlet pressure gradient and also contribute weakly to the differences between the development of the secondary flows for the investigated configurations.

Conf.	$\beta_{1steady} - \beta_1$	$\frac{Tu_1}{Tu_{1steady}}$	$\frac{p_{t1}}{p_{t1steady}}$
steady	0°	1	1
T40 10	2.5°	1.29	0.993
T40 20	3.2°	1.44	0.993
T80 20	1.3°	1.01	0.996
T80 40	2.1°	1.20	0.994
T80 80	3.7°	1.62	0.992

Table 2: **Time-averaged cascade inlet values in measurement plane 1**

Conf.	St.dev.	Max	Min
steady	5.44	31.7	-46.9
T40 10	4.31	26.3	-40.0
T40 20	3.73	22.7	-33.0
T80 20	4.78	22.0	-40.1
T80 40	3.37	16.2	-22.2
T80 80	3.32	17.8	-25.4

Table 3: **Time-averaged predicted SVO_n distribution values in measurement plane 2**

In order to better understand the differences between the investigated configurations, in Fig. 8 the time-averaged entropy generation values and the streamlines are visualised on the blade suction surfaces. In the pictures the flow direction is from left to right, consequently leading edge (L.E.) is on the left boundary and trailing edge (T.E.) on the right. The highest entropy generation values are near the endwall where the passage vortex interacts with the suction surface. For the steady configuration a long separation bubble with reattachment is identified by the streamlines in the midspan region, which becomes smaller for the time-averaged values of the T80 20 configuration. For the other four unsteady configurations the separation bubble in the midspan region is not visible any more, probably due to the higher average inlet turbulence level (Tab. 2) considering one domain passing period, and the streamlines near the trailing edge region become more parallel. The presence of the suction surface separation bubble seems to play an important rule for the development of the secondary flow downstream the trailing edge in low pressure turbine profiles. Its presence seems to influence partially the intensity of the trailing edge wake vortex, consequently the span-wise position and intensity of the

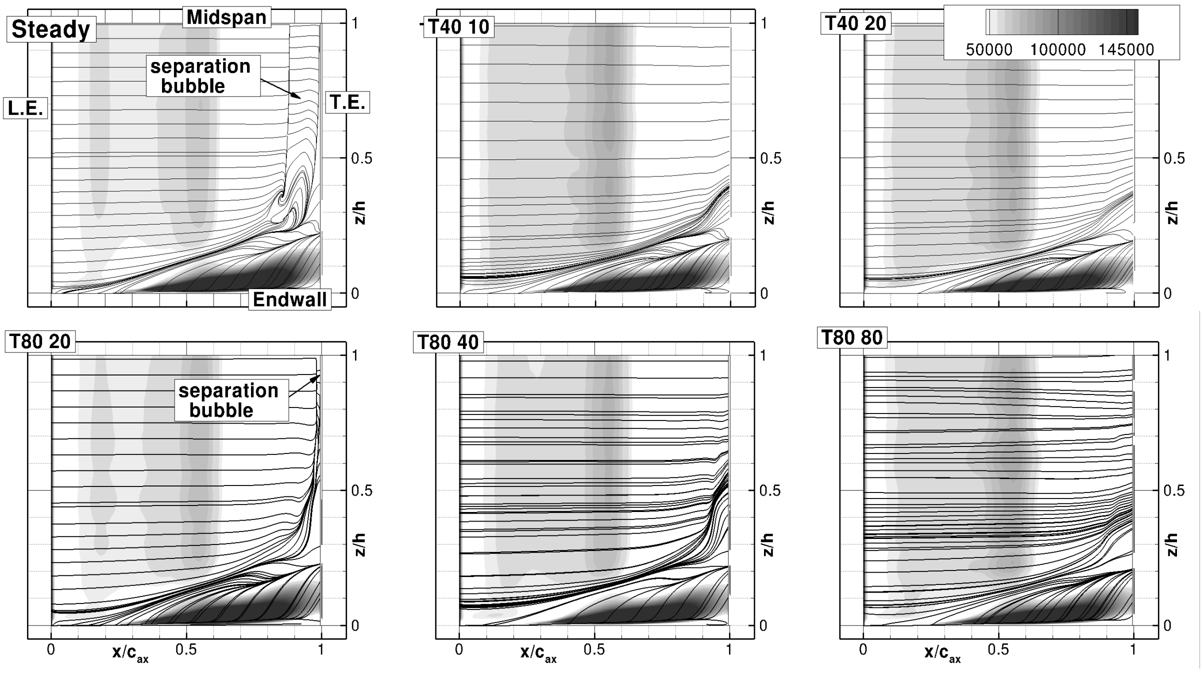

Figure 8: **Time-averaged entropy generation and streamlines near (3th node level from the surface) the blade suction surface.**

SVO_n, like observed in Fig. 7. The formation of a vortex (TEWV) of significant proportions which contains the trailing shed vorticity is consequently influenced by the flow behaviour on the blade suction surface near the trailing edge and by the period(e)-238.542(b)-1salin

All the unsteady configurations are characterised by a relative small inlet boundary layer and consequently weak secondary flows. The variation of the cascade inflow angle and of the inlet turbulence level for the unsteady configurations cause a reduction of the secondary streamwise vorticity SVO_n in the plane 40% chord length downstream the cascade, with increase of the bar passing frequency. Moreover, for the investigated configurations, the increase of the time-averaged inlet turbulence influences the suction surface transition behaviour near the trailing edge and consequently the interaction between the secondary flow development and the suction surface in this region. Downstream the investigated aft loaded LPT cascade, this results in weaker secondary streamwise vorticity SVO_n.

ACKNOWLEDGEMENTS

The investigations were conducted as a part of the Deutsche Forschungsgemeinschaft joint research project PAK-530. The authors wish to acknowledge DLR Cologne, Institute of Propulsion Technology, for provision of the numerical flow solver TRACE and for the useful collaboration.

REFERENCES

Acton, P., (1998), *"Untersuchungen des Grenzschichtumschlages an einem hochbelasteten Turbinengitter unter inhomogenen und instationaeren Zustroembedingungen "*, Ph.D.thesis. Universitaet der Bundeswehr Muenchen.

Ainsworth, R. W., Allen, J. L., Dietz, A. J., (1989), *"Methods for Making Unsteady Aerodynamic Pressure Measurements in a Rotating Turbine Stage "*, AGARD CP.468, pp. 22/1-22/13

Casciaro, C., Treiber, M., Sell, M., (2000), *"Unsteady Transport Mechanisms in an Axial Turbine"*, ASME Paper GT2000-0440.

Ciorciari, R., Kirik, I., Niehuis, R., (2014), *"Effects of Unsteady Wakes on the Secondary Flows in the Linear T106 Turbine Cascade"*, J. Turbomach. 136(9).

Coton, T., (2004), *"Unsteady Wake-Boundary Layer Interaction on Advanced High Lift Low Pressure Turbine Aitfoils"*, Ph.D.thesis. Von Karman Institute for Fluid Dynamics.

Dring, R.P., Joslyn, H.D., Hardin, L.W., Wagner, J.H., (1982), *"Turbine Rotor-Stator Interaction "*, Journal of Engineering for Power, Vol. 104, pp. 729-742.

Duden, A., (1999), *"Stroemungsbeeinflussung zur Reduzierung der Sekundaerstroemungen in Turbinengittern"*, Ph.D.thesis. Universitaet der Bundeswehr Muenchen.

Engel, K., (1997), *"Numerische Simulation der instationaeren Stroemung in Turbomaschinenkomponenten"*, Ph.D.thesis.Universitaet Gesamthochschule Essen.

Eulitz, F., (2000), *"Numerische Simulation und Modellierung der instationaeren Stroemung in Turbomaschinen"*, Ph.D.thesis. Ruhr-Universitaet Bochum.

Hodson, H. P. and Dominy, R. G. (1987), *"Three-Dimensional Flow in a Low Pressure Turbine Cascade at its Design Conditions "*, J. Turbomach. 109, pp. 177-185

Hodson, H. P., and Howell, R. J., (2005), *"Blade-row interactions, transiton, and high-lift aerfoils in low-pressure turbines "*, Annu. Rev. Fluid Mech. 2005, 37, pp. 71-98.

Kato, M., and Launder, B., (1993), *"The modelling of turbulent flow around stationary and vibrating square cylinders"*, 9th Turbulent Shear Flow Symposium, Kyoto, Japan.

Kirik, I., Niehuis, R., (2015) *"Experimental Investigation on Effects of Unsteady Wakes on the Secondary Flows in the Linear T106 Turbine Cascade"*, ASME Paper GT2015-43170 (to be published)

Kozulovic, D., Roeber, T., Kuegeler, E., Nuernberger, D., (2004), *"Modifications of a two-equation turbulence model for turbomachinery fluid flows"*, Deutscher Luft- und Raumfahrtkongress, Dresden, Germany.

Ladwig, M., (1991), *"Experimentelle Untersuchungen zum Einfluß einer inhomogener Zustroemung auf die Entwicklung des Stroemungsfeldes in Turbinenschaufelgittern"*, Ph.D.thesis. Universitaet der Bundeswehr Muenchen.

Lampart, P., (2009 a), *"Investigation of Endwall Flows and Losses in Axial Turbines. Part I. Formation of Endwall Flows and Losses "*, J. of Theoretical and Applied Mechanics, 47(2), pp. 321-342.

Lampart, P., (2009 b), *"Investigation of Endwall Flows and Losses in Axial Turbines. Part II. The Effect of Geometrical and Flow Parameters "*, J. of Theoretical and Applied Mechanics, 47(2), pp. 321-342.

Lakshminarayana, B., Poncet, A., (1974), *"A Method of Measuring Three-Dimensional Rotating Wakes behind Turbomachines"*, J. of Fluids Engineering, 96(2), pp. 87-91.

Marciniak, V., Kuegeler, E., Franke, M., (2010), *"Predicting transition on low-pressure turbine profiles "*, Fifth European Conference on Computational Fluid Dynamics ECCOMAS CFD 2010, Lisbon, Portugal

Pacciani, R., Marconcini, M., Arnone, A.,Bertini, F., (2012), *"URANS Analysis of wake-induced effects in High.Lift, Low Reynolds Number Cascade Flows"*, ASME Paper GT2012-69479.

Reinmoeller, U., Stephan,B., Schmidt, S., Niehuis, R., (2002), *"Clocking effects in a 1.5 Stage Axial Turbine-Steady and Unsteady Experimental Investigations Supported by Numerical Simulations "*, J. Turbomach. 124, January 2002.

Reinmoeller, U.,(2007), *"Experimentelle Untersuchungen von instationaeren Stroemungsphaenomenen in Axialturbinen "*, Ph.D.thesis. RWTH-Aachen.

Renaud, E. W., (1991), *"Secondary Flow, Total Pressure Loss and the Effect of Circumferential Distorsions in Axial Turbine Cascades "*, Ph.D.thesis. Massachusetts Institute of Technology.

Rose, M., Schupbach, P., Mansour, M., (2013), *"The Thermodynamics of Wake Blade Interaction in Axial Flow Turbines: Combined Experimental and Computational Study "*, J. Turbomach. 135.

Schobeiri, M. T., Oeztuerk, B., Ashpis, D. E., (2003), *"On the physics of the flow separation along a low pressure turbine blade under unsteady flow conditions"*, ASME Paper GT2003-38917.

Schwarze, M., and Niehuis, R., (2010). *"Numerical simulation of a highly loaded LPT cascade with strong suction side separation under periodically unsteady inflow conditions"*, ASME Paper GT2010-22363.

Stadtmueller, P., (1999), *"Grenzschichtentwicklung und Verlustverhalten von hochbelasteten Turbinengittern unter Einfluß periodisch instationaerer Zustroemung "*, Ph.D.thesis. Universitaet der Bundeswehr Muenchen.

Sturm, W. and Fottner, L. (1985), *"The High-Speed Cascade Wind Tunnel of the German*